Interface properties of an oxidised Au/Ni/AlGaN MIS structure

M J Legodi[1], **W E Meyer and F D Auret**
Department of Physics, University of Pretoria, Private Bag X20, Hatfield 0028

E-mail: matshisa.legodi@up.ac.za

Abstract. In the analysis of current-voltage measurements on Schottky barrier diodes, the thermionic emission (*TE*) model is routinely employed. In this scheme, the Schottky barrier height (SBH) and the ideality factor (n) are assumed to be the same throughout the metal-semiconductor contact and to be independent of measurement temperature. We examine these assumptions in the context of an oxygen annealed Au/Ni/AlGaN MIS structure and find the assumptions inadequate in the temperature range 60 K – 330 K. Our measurements reveal that, the SBH and n increase (0.20 eV – 0.81 eV) and decrease (4.38 – 1.37) respectively, with increasing temperature. When a model that assumes a distribution of SBH in the barrier is used to analyse the Au/Ni/AlGaN structure, the SBH is found to follow a distinct Gaussian distribution above and below 180 K, with: $\Phi(T>180\ \text{K})=1.123$ eV and $\sigma = 0.002$ eV; and, $\Phi(T<180\ \text{K})=0.580$ eV and $\sigma = 0.004$ eV, respectively. Current transport is thermionic-field-emission (*TFE*) below 180 K and thermionic-emission (*TE*) with a "T_0 anomaly" above 180 K.

1. Introduction

Stable Schottky barrier contacts have been reported for metal-insulator-semiconductor (MIS) structures with the dielectric ranging from leaky to insulating [1-5]. One way to tailor the response of FETs is by sandwiching dielectric between the gate metal and the semiconductor, for example, in MOSFETs and IGFETs. Some dielectrics passivate defects at the semiconductor surface or may have defects embedded within that communicate with the semiconductor surface states and may affect device properties [5].

Φ_B and n for devices operating in extended temperature ranges can exhibit anomalous behavior inconsistent with thermionic-emission theory (*TE*). Some workers [5-7] attribute the anomalous behavior to the presence of Schottky barrier inhomogeneities in the interface. The origins of these inhomogeneities could be as diverse as non-uniformity and defects in the oxide layer to lack of stoichiometry at the semiconductor surface. In this study, we analyze Au/Ni/$Al_{0.18}Ga_{0.82}N$ Schottky contacts oxidized at temperatures up to 573 K. We also study current transport across the diode over a wide temperature range to establish the primary conduction mechanisms. Lastly, analyzing the *I–V–T* data, we use a model that assumes a Gaussian distribution of Schottky barriers in the interface to explain the observed abnormalities.

[1] To whom any correspondence should be addressed.

2. Experimental details

0.6 µm thick $Al_{0.18}Ga_{0.82}N$ layers, hydride vapour-phase epitaxially (*HVPE*) grown with free carrier density 2.12×10^{18} cm^{-3} were studied. *I–V–T* measurements were performed in a closed-cycle liquid Helium cryostat capable of better than 50 mK stability. An HP 4140B picoammeter / DC supply was utilised for the *I–V* measurements. Ti/Al/Ni/Au ohmic contacts were deposited on the epi-layers and a 20 nm Ni Schottky contact layer followed by a 50 nm Au capping layer were resistively evaporated after oxide removal in H_2O:HCL solution. Annealing was carried out in a tube furnace for 30 minute periods in flowing Oxygen.

3. Results and Discussions

The thermionic-emission-tunnelling [8-9] current through a Schottky diode is:

$$I = SA^{**}T^2 \exp\left(\frac{-q\Phi_B}{k_B T}\right)\left[\exp\left(\frac{q(V-IR_S)}{nk_B T}\right)-1\right] + \frac{SA^{**}T^2}{\alpha}\left[\exp\left(\frac{-q\Phi_B}{k_B T}\right)\exp\left(\frac{qV}{k_B T}\right)-\exp\left(\frac{-q\Phi_B}{E_{00}}\right)\exp\left(\frac{qV}{E_{00}}\right)\exp\left(\alpha\frac{qV_n}{E_{00}}\right)\right] \quad (1)$$

where $\alpha = (k_B T/E_{00})-1$. The saturation currents for thermionic and for tunnelling are:

$$I_0 = SA^{**}T^2\exp(-q\Phi_B/k_B T) \text{ and } I_0' = SA^{**}T^2\exp(-q\Phi_B/E_{00})\exp(qV_n/k_B T). \quad (2)$$

In equation (2), Φ_B is the Schottky barrier height (SBH), E_{00}, the characteristic energy and qV_n, the bulk Fermi level position. *n*, is the ideality factor, A^{**}, the effective Richardson constant, *S* the contact area and R_S, the series resistance. Equation (1) tends to the familiar *TE* limiting case: $I = I_0\exp\left[\left(q(V-IR_S)/nk_B T\right)-1\right]$ when $E_{00} << k_B T$. When $E_{00} >> k_B T$, the tunnelling component dominates, and equation (1) reduces to: $I = I_0'\exp(qV/E_{00})$. The slope, E_{00}, and Φ_B can be determined from equation (2) while the ideality factor, *n*, is determined from a linear fit to the forward part of the semi-log *I–V* characteristics through: $n = (q/k_B T)\,\mathrm{d}\ln(V-IR_S)/\mathrm{d}\ln I$. An activation plot of ln (I_0/ST^2) vs $1/T$ –the Richardson plot– is used to determine Φ_B and A^{**}.

Figure 1 is the forward *I–V* characteristics of the AlGaN sample (a) immediately after oxidation and, (b) two weeks after exposure to ambient air and temperature, nominally 298 K. The as deposited (300 K) and the 373 K oxygen annealed. Log (*I*)–*V* plots in figure 1 (a) are co-incident and are reasonably linear over a few orders of magnitude. After 573 K oxidation, a current plateau develops at low voltages indicating a turn-on voltage of about 0.4 V indicating the presence of insulating NiO and thus a MIS structure [10-11]. Upon re-measuring the 573 K samples, we noted the *I–V* characteristics had evolved to the 300 K plot in figure 1(b). The formation of the NiO and its evolution are subjects of an on-going study in our laboratory.

AlGaN has a high density of dislocation defects and our samples are highly doped (2.12×10^{18} cm^{-3}) leading to a high tunnelling probability. We believe the *leaky* NiO layer is occasioned by charge re-distribution increasing the tunnelling current. Evidence in support is the near disappearance of the turn-on voltage, the large increase ($<10^{-10}$ A to ~10^{-8} A) in the reverse leakage current, the decrease in Φ_B from 1.308 eV to 0.726 eV and the nearly temperature-independent slopes of *I–V–T* plots in figure 1(b), indicative of defect-assisted tunnelling [8].

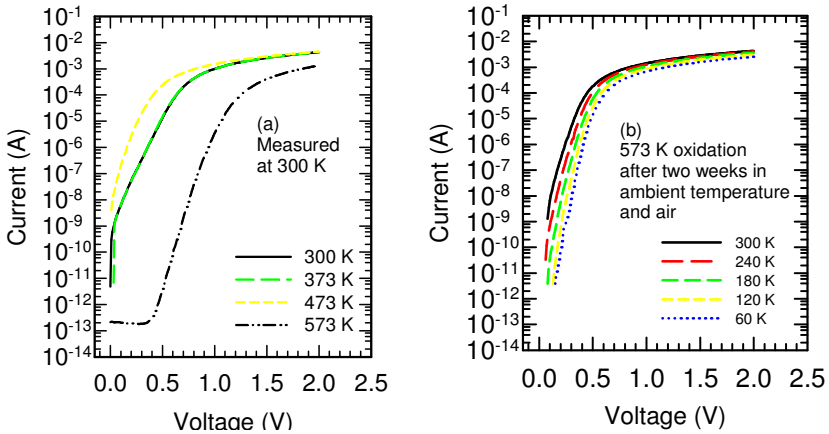

Figure 1. (a) Forward *I–V* plots of un-annealed (300 K), 373 K, 473 K and 573 K oxidized Au/Ni/$Al_{0.18}Ga_{0.82}N$ diodes. The 573 K plot shows a turn-on voltage at 0.4 V indicative of the insulating NiO in the interface. These plots were recorded at 300 K. (b) Selected forward *I–V–T* plots of the 573 K Au/Ni/$Al_{0.18}Ga_{0.82}N$ diode measured between 330 K and 60 K. The *I–V* plots have almost the same slope and are closely spaced indicative of tunnelling.

Table 1 summarizes *I–V* parameters before and after oxidation. Oxidizing the Ni/Au contact at 373 K, 473 K and 573 K clearly improves its rectifying characteristics. Although $\Phi_B(I-V)$ increases from 0.644 eV to 1.308 eV corresponding to oxidation temperatures 300 K and 573 K, $\Phi_B(I-V)$ subsequently reduces to 0.767 eV after exposure to ambient air and temperature, as shown in figure 1. The remainder of results herein pertain to the Au/Ni/$Al_{0.18}Ga_{0.82}N$ of figure 1(b).

Table 1. Au/Ni/$Al_{0.18}Ga_{0.82}N$ *I–V* characteristics before and after oxidation up to 573 K.

T (K)	*n*	Φ_B (I-V) (eV)	I_R (at –1V) (A)
300	2.09	0.644	4.80×10^{-08}
373	1.95	0.654	3.45×10^{-08}
473	1.39	0.589	1.99×10^{-07}
573	1.26	1.308	$<10^{-10}$
573[$]	1.27	0.762	1.07×10^{-08}

[$] Re-measured after exposure to ambient air and temperature for two weeks.

Real Schottky contacts like those in figure 2, are sensitive to details of the interface in metal-semiconductor (M-S) systems [12-16]. The concept of spatially inhomogenous potentials in M-S systems is useful for understanding abnormal *I–V–T* parameters [17-21]. In figure 2, Φ_B decreases with decreasing temperature while *n* increases. This behaviour is indicative of an inhomogenous spatial distribution of the potential in the interface. The Richardson plot (not shown) of ln (I_0/ST^2) vs $1/T$ for Au/Ni/$Al_{0.18}Ga_{0.82}N$ is non-linear at low temperatures, implying temperature-dependent Φ_B and *n*. The A^{**} determined from the linear part is very small compared to the theoretical $A^{**} = 4\pi m_e^* q k_B^2 / h^3 = 29$ A cm^{-2} K^{-2}. Re-plotting ln (I_0/AT^2) vs $1/nT$ as described in [22] and later [23] to ameliorate effects of the temperature dependent Φ_B, yields a linear plot. However, the extracted Φ_B and A^{**} are still too small.

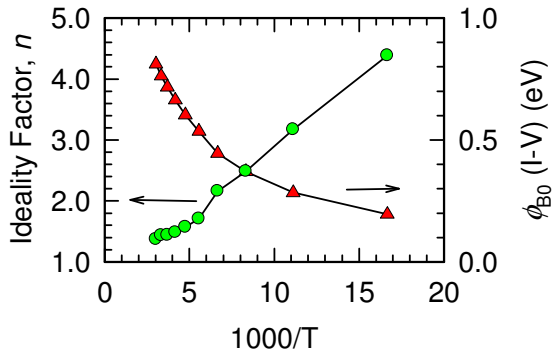

Figure 2. Au/Ni/$Al_{0.18}Ga_{0.82}N$ anomalous SBH and n vs $10^3/T$ measured between 330 K and 60 K.

Extracting the intercepts on the Φ_B axis at n = 1 yields homogenous SBHs: $\Phi_B^{T<180K} = 0.54\,\text{eV}$ and $\Phi_B^{T>180K} = 1.09\,\text{eV}$.

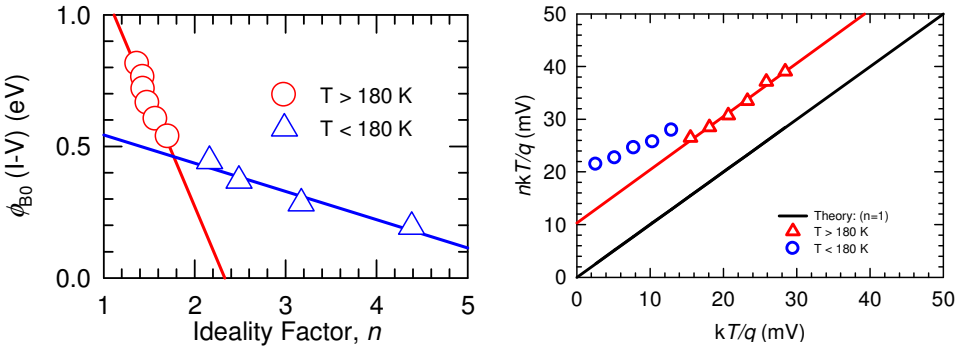

Figure 3. (a) The effective Φ_B vs n indicating two linear regimes around T = 180 K. (b) nk_BT/q vs k_BT/q for Au/Ni/$Al_{0.18}Ga_{0.82}N$. Open triangle symbols show the "T_0 anomaly" for T > 180 K and the open circles show *TFE* for T > 180 K. The theory line (n = 1) indicates pure *TE*.

According to Padovani and Stratton [24] and [9], tunnelling dominates current transport in moderate-to-heavily doped devices that operate at low temperatures.. Our results of nk_BT/q vs k_BT/q in figure 3(b) suggest thermionic-field-emission (*TFE*) for T < 180 K. The "T_0 anomaly" shown by Werner *et al* [16] to originate from the temperature and voltage dependence of n and Φ_B is caused by spatial inhomogeneities in the Schottky junction.

Tung [17], Sullivan *et al* [25] and, Werner and Guttler [16], have developed analytical models for the spatial distribution of the potential. Assuming a Gaussian distribution of barrier heights we write the following probability for each Schottky barrier height in the distribution:

$$P(\Phi_B) = \left(1/\sigma_S\sqrt{2\pi}\right)\exp\left[-\left(\Phi_B - \bar{\Phi}_{B0}\right)^2/2\sigma_S^2\right] \qquad (3)$$

where, $\bar{\Phi}_{B0}$ and σ_S are respectively, the distribution's mean barrier height and standard deviation. We integrate over all spatially distributed barriers to get the total current through the barrier contact. The *TE* equation is re-written in terms of the Gaussian distribution parameters as:

$$I = SA^{*}T^{2}\exp\left[-\frac{q}{k_{\mathrm{B}}T}\left(\bar{\Phi}_{B0}-\frac{q\sigma_{S}^{2}}{2k_{\mathrm{B}}T}\right)\right]\exp\left(\frac{qV}{n_{ap}k_{\mathrm{B}}T}\right)\left[1-\exp\left(-\frac{qV}{k_{\mathrm{B}}T}\right)\right] \quad (4)$$

where $\Phi_{ap} = \bar{\Phi}_{\mathrm{B0}}(T=0) - \frac{q\sigma_{S}^{2}}{2k_{\mathrm{B}}T}$ and $\frac{1}{n_{ap}} - 1 = \rho_2 - \frac{\rho_3}{2k_{\mathrm{B}}T}$. (5)

In this scheme, the voltage coefficients, ρ_2 and ρ_3, describe the voltage-deformation of the Gaussian distribution and are related to the distribution parameters by: $\bar{\Phi}_{\mathrm{B}} = \bar{\Phi}_{\mathrm{B0}} + \rho_2 V$ and $\sigma_{\mathrm{S}} = \sigma_{\mathrm{S0}} + \rho_3 V$.

Figure 6 shows (a) Φ_{ap} vs $1/(2k_{\mathrm{B}}T)$ and (b) $(1/n_{\mathrm{ap}} - 1)$ vs $1/(2k_{\mathrm{B}}T)$ plots respectively, utilized to determine $\bar{\Phi}_{\mathrm{B}}$, the mean SBH i.e. the barrier height at $T = 0$, σ_{S}, the standard deviation and the voltage-deformation coefficients ρ_2 and ρ_3 of the Gaussian distribution of the SBHs. It is evident throughout our discussions that there are two distinct regimes, centred on $T = 180$ described by two Gaussian distributions. The $T > 180$ K regime is described by a higher mean SBH, $\bar{\Phi}_{\mathrm{B}}^{T>180\,\mathrm{K}} = 1.12$ eV and a standard deviation, $\sigma_{\mathrm{S}}^{T>180\,K} = 0.136$ eV; and a lower mean SBH, $\bar{\Phi}_{\mathrm{B}}^{T<180\,\mathrm{K}} = 0.580$ eV and $\sigma_{\mathrm{S}}^{T<180\,K} = 0.0643$ eV. These distributions correspond to the dominance of the *TE* and *TFE* conduction mechanisms. At low temperatures, the electric field due to the ionized donors ensure the charge carriers "see" a thinner and lower SBH, enhancing current flow, while at higher temperatures more charges have the requisite energy to surmount higher SBHs. Also, $\rho_3 \sim 10^{-3}$ is very small during *TE* and *TFE* thus has little influence on the SBH. However, ρ_2, with magnitudes 0.11 and 0.40 is significant.

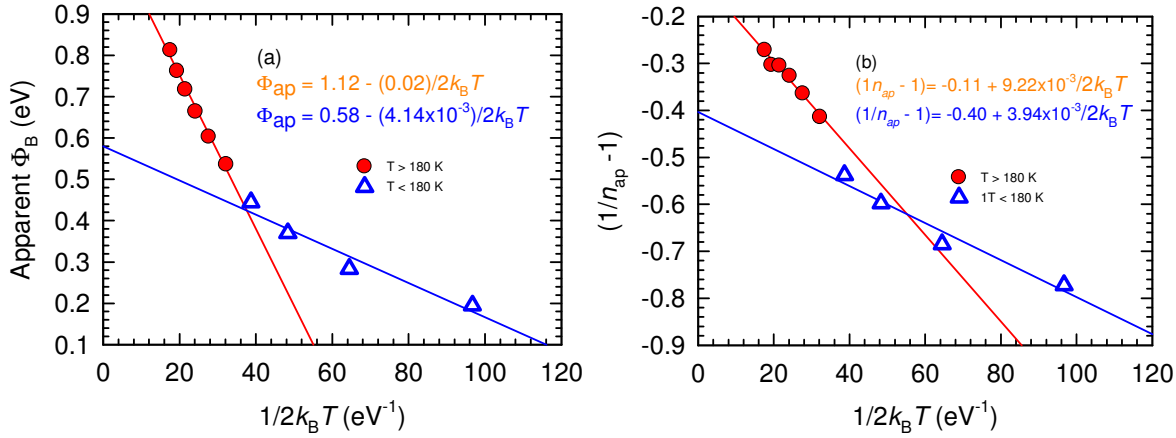

Figure 6. (a) Φ_{ap} vs $1/(2k_{\mathrm{B}}T)$ and (b) $1/n_{\mathrm{ap}} - 1$ vs $1/(2k_{\mathrm{B}}T)$ plots utilized to determine $\bar{\Phi}_{\mathrm{B}}$, the mean SBH i.e. the barrier height at $T = 0$, σ_{S}, the standard deviation and the voltage-deformation coefficients ρ_2 and ρ_3.

4. Conclusions

Oxidation improves rectifying characteristics of Au/Ni/$Al_{0.18}Ga_{0.82}N$ and forms a MIS structure with NiO the insulating layer. The *I–V–T* derived *n* and Φ_{B} of the MIS are temperature-dependent and anomalous. A Gaussian distribution model for Φ_{B} describes current transport: *TE* regime has $\bar{\Phi}_{\mathrm{B}}^{T>180\,\mathrm{K}} = 1.12$ eV and $\sigma_{\mathrm{S}}^{T>180\,K} = 0.136$ eV; while the *TFE* regime has $\bar{\Phi}_{\mathrm{B}}^{T<180\,\mathrm{K}} = 0.580$ eV and $\sigma_{\mathrm{S}}^{T<180\,K} = 0.0643$ eV.

Acknowledgments

The financial assistance of the South African National Research Foundation is acknowledged.

5. References

[1] M. Ozer, D. E. Yıldız, S. Altundal, and M. M. Bulbul, "Temperature dependence of characteristic parameters of the Au/ SnO2/n-Si (MIS) Schottky diodes," *Solid-State Electronics*, vol. 51, pp. 941-949, 2007.

[2] C. H. Lan et al., "(NH$)2Sx-treated AlGaN MIS photodetectors with LPD SiO2 layer," *Journal of the Electrochemical Society*, vol. 157, no. 6, pp. 613-616, 2010.

[3] C.-T. Lee, "GaN-based metal-oxide-semiconductor devices," in *Semiconductor Technologies*, Taiwan: , 2008, pp. 151-208.

[4] S. K. Zhang, Z. W. Fu, L. Ke, F. Lu, Q. Z. Qin, and X. Wang, "Properties of interface states at Ta2O5/n-si interfaces," *Journal of Applied Physics*, vol. 84, no. 1, pp. 335-338, 1998.

[5] H. Rohdin, N. Moll, A. M. Bratkovsky, and C. Su, "Dispersion and tunneling analysis of the interfacial gate resistance in Schottky barriers," *Physical Review B*, vol. 59, no. 20, pp. 102-113, 1999.

[6] T. H. DiStefano, "Barrier Inhomogeneities on a Si/SiO2 Interface by Scanning Internal Photoemission," *Applied Physics Letters*, vol. 19, no. 8, p. 280, 1971.

[7] G. S. Lujan et al., "Interface Passivation Mechanisms in Metal Gated Oxide Capacitors," in *Proceeding of the 34th European Solid-State Device Research conference, 2004. ESSDERC 2004*, 2004, pp. 325-328.

[8] L. S. Yu, Q. Z. Liu, D. J. Qiao, S. S. Lau, and J. Redwing, "The role of the tunneling component in the current-voltage characteristics of metal-GaN Schottky diodes," *Journal of Applied Physics*, vol. 84, no. 4, pp. 2099-2104, 1998.

[9] S. M. Sze, *Physics of Semiconductors*, 2nd ed. New Jersey: John Wiley & Sons, 1981.

[10] B. Sasi and K. G. Ã. Gopchandran, "Preparation and characterization of nanostructured NiO thin films by reactive-pulsed laser ablation technique," *Solar Energy Materials*, vol. 91, pp. 1505-1509, 2007.

[11] F. D. Auret, L. Wu, W. E. Meyer, J. M. Nel, M. J. Legodi, and M. Hayes, "No Title," *Physica Status Solidi (C)*, vol. 1, no. 4, p. 674, 2004.

[12] J. Bardeen, "Surface states and rectification at a metal semiconductor contact," *Physical Review*, vol. 71, no. 10, pp. 717-727, 1947.

[13] F. Roccaforte, F. Giannazzo, F. Iucolano, J. Eriksson, M. H. Weng, and V. Raineri, "Applied Surface Science Surface and interface issues in wide band gap semiconductor electronics," *Applied Surface Science*, vol. 256, no. 19, pp. 5727-5735, 2010.

[14] L. Boussouar, Z. Ouennoughi, N. Rouag, A. Sellai, R. Weiss, and H. Ryssel, "Investigation of barrier inhomogeneities in Mo/4H–SiC Schottky diodes," *Microelectronic Engineering*, vol. 88, no. 6, pp. 969-975, 2011.

[15] S. Ashok, J. M. Borrego, and R. J. Gutmann, "Electrical characteristics of GaAs MIS Schottky diodes," *Solid-State Electronics*, vol. 22, pp. 621-631, 1979.

[16] J. H. Werner and H. H. Güttler, "Barrier inhomogeneities at Schottky contacts," *Journal of Applied Physics*, vol. 69, no. 3, 1991.

[17] R. T. Tung, "Electron transport in metal-semiconductor interfaces: General theory," *Physical Review B*, vol. 45, no. 23, pp. 13509-13523, 1992.

[18] S. Asubay, O. Gullit, and A. Turut, "Determination of the laterally homogeneous barrier height of metal / p-InP Schottky barrier diodes," *Vacuum*, vol. 83, pp. 1470-1474, 2009.

[19] H. Dogan, H. Korkut, N. Yıldırım, and A. Turut, "Prediction of lateral barrier height in identically prepared Ni / n-type GaAs Schottky barrier diodes," *Applied Surface Science*, vol. 253, pp. 7467-7470, 2007.

[20] K. Sarpatwari, O. O. Awadelkarim, M. W. Allen, S. M. Durbin, and S. E. Mohney, "Extracting the Richardson constant: IrO2/n-ZnO Schottky diodes," *Applied Physics Letters*, vol. 94, pp. 1-3, 2009.

[21] K. Sarpatwari, S. E. Mohney, and O. O. Awadelkarim, "Effects of barrier height inhomogeneities on the determination of the Richardson constant," *Journal of Applied Physics*, vol. 109, pp. 1-7, 2011.

[22] A. N. Saxena, "Forward curent-voltage characteristics of Schottky barriers on n-type Silicon," *Surface Science*, vol. 13, pp. 151-171, 1969.

[23] R. F. Schmitsdorf, T. U. Kampen, and W. Monch, "Explanation of the linear correlation between barrier heights and ideality factors of real MS contacts by laterally nonuniform Schottky barriers," *J. Vac. Sci Technol. B*, vol. 15, no. 4, pp. 1221-1226, 1997.

[24] F. A. Padovani and R. Stratton, "Field and emission in Schottky barriers," *Solid-State Electronics*, vol. 9, pp. 695-707, 1966.

[25] J. P. Sullivan, R. T. Tung, M. R. Pinto, and W. R. Graham, "Electron transport of inhomogeneous Schottky barriers: A numerical study," *Journal of Applied Physics*, vol. 70, no. 12, 1991.